Upper-Ocean Thermal Structure and the Western North Pacific Category 5 Typhoons. Part II: Dependence on Translation Speed

I.-I. LIN, IAM-FEI PUN, AND CHUN-CHIEH WU

Department of Atmospheric Sciences, National Taiwan University, Taipei, Taiwan

(Manuscript received 8 July 2008, in final form 9 December 2008)

ABSTRACT

Using new in situ ocean subsurface observations from the Argo floats, best-track typhoon data from the U.S. Joint Typhoon Warning Center, an ocean mixed layer model, and other supporting datasets, this work systematically explores the interrelationships between translation speed, the ocean's subsurface condition [characterized by the depth of the 26°C isotherm (D26) and upper-ocean heat content (UOHC)], a cyclone's self-induced ocean cooling negative feedback, and air–sea enthalpy fluxes for the intensification of the western North Pacific category 5 typhoons. Based on a 10-yr analysis, it is found that for intensification to category 5, in addition to the warm sea surface temperature generally around 29°C, the required subsurface D26 and UOHC depend greatly on a cyclone's translation speed. It is observed that even over a relatively shallow subsurface warm layer of D26 ~ 60–70 m and UOHC ~ 65–70 kJ cm^{-2}, it is still possible to have a sufficient enthalpy flux to intensify the storm to category 5, provided that the storm can be fast moving (typically U_h ~ 7–8 m s^{-1}). On the contrary, a much deeper subsurface layer is needed for slow-moving typhoons. For example at U_h ~ 2–3 m s^{-1}, D26 and UOHC are typically ~115–140 m and ~115–125 kJ cm^{-2}, respectively. A new concept named the affordable minimum translation speed $U_{h\_\min}$ is proposed. This is the minimum required speed a storm needs to travel for its intensification to category 5, given the observed D26 and UOHC. Using more than 3000 Argo in situ profiles, a series of mixed layer numerical experiments are conducted to quantify the relationship between D26, UOHC, and $U_{h\_\min}$. Clear negative linear relationships with correlation coefficients $R = -0.87$ (-0.71) are obtained as $U_{h\_\min} = -0.065 \times \text{D26} + 11.1$, and $U_{h\_\min} = -0.05 \times \text{UOHC} + 9.4$, respectively. These relationships can thus be used as a guide to predict the minimum speed a storm has to travel at for intensification to category 5, given the observed D26 and UOHC.

1. Introduction

a. Motivation

Category 5[1] tropical cyclones are the most intense and damaging cyclones on earth. Why these storms can reach such extraordinary intensity has been an intriguing and challenging research topic because intensification is a complex process involving multiple interactions among the cyclone, ocean, and atmosphere (Gray 1977; Merrill 1988; Emanuel 1995, 1997, 1999, 2005; Shay et al. 2000; Frank and Ritchie 2001; Emanuel et al. 2004; Lin et al. 2005, 2008, 2009; Trenberth 2005; Montgomery et al. 2006; Houze et al. 2007; Vimont and Kossin 2007; Black et al. 2007; Vecchi and Soden 2007; Wu et al. 2007; Mainelli et al. 2008). To reach such high intensity, multiple conditions of both atmosphere (e.g., vertical wind shear and high level outflow; Frank and Ritchie 2001; Wang and Wu 2003; Emanuel et al. 2004) and ocean all have to be favorable. Also, since ocean is the energy source for intensification, it is a necessary condition (Emanuel 1995, 1997, 1999; Shay et al. 2000; Emanuel et al. 2004; Lin et al. 2005, 2008, 2009; Trenberth 2005; Black et al. 2007). Thus, even if all other conditions are favorable, without satisfying the ocean condition it is not possible for the intensification to take place.

When considering the ocean condition, both sea surface temperature (SST) and the subsurface thermal structure are important because cyclones interact not only with

[1] Saffir–Simpson tropical cyclone scale based on the 1-min (10 min) maximum sustained winds—category 1: 34–43 (30–37) m s^{-1}, category 2: 44–50 (38–43) m s^{-1}, category 3: 51–59 (44–51) m s^{-1}, category 4: 59–71 (52–61) m s^{-1}, and category 5: >71 (>61) m s^{-1}.

Corresponding author address: Dr. I.-I. Lin, Dept. of Atmospheric Sciences, National Taiwan University, No. 1, Sec. 4, Roosevelt Rd., Taipei 106, Taiwan.
E-mail: iilin@as.ntu.edu.tw

DOI: 10.1175/2009MWR2713.1

the ocean surface, but also with the entire upper-ocean column (typically from surface down to 100–200 m; Perlroth 1967; Leipper and Volgenau 1972; Gray 1979; Holliday and Thompson 1979; Shay et al. 2000; Cione and Uhlhorn 2003; Goni and Trinanes 2003; Lin et al. 2005, 2008, 2009; Pun et al. 2007; Wu et al. 2007). However, the lack of subsurface observations has long been a major hindrance to understand the role the ocean's subsurface thermal structure plays in the intensification of category 5 cyclones.

In recent years, because of the advancement in ocean in situ observations (e.g., the deployment of Argo floats; Gould et al. 2004; Roemmich et al. 2004), the situation has improved and new observations are now available for research (Johnson et al. 2006; Lyman et al. 2006; Trenberth 2006; Willis et al. 2007). Therefore in Lin et al. (2008, hereafter Part I) of this work, these new subsurface observations are used to explore issues related to ocean features, while in this work (Part II) the focus is on exploring issues related to cyclone's translation speed. As in Part I, western North Pacific typhoons are studied because this area is where most category 5 cyclones occur on earth.

b. Issues on the translation speed

In the extant literature, it is generally known that if a cyclone is to reach a high intensity such as category 5, in addition to warm SST, a sufficiently thick layer of warm water below the surface is required as a necessary precondition (Leipper and Volgenau 1972; Gray 1979; Holliday and Thompson 1979; Emanuel 1999; Shay et al. 2000; Cione and Uhlhorn 2003; Emanuel et al. 2004; Lin et al. 2005; Part I). This is required because it will ensure that the negative feedback from the cyclone's self-induced SST cooling is restrained during the intensification. Otherwise, the self-induced cooling would be too strong for continual intensification to category 5 since self-induced cooling reduces the available air–sea flux supply for intensification (Price 1981; Gallacher et al. 1989; Emanuel 1999; Cione and Uhlhorn 2003; Emanuel et al. 2004; Lin et al. 2005, 2009; Part I; Wu et al. 2007). As reported in Gallacher et al. 1989, Emanuel (1999), and Emanuel et al. (2004), a mere 2.5°C cooling in the inner core is already sufficient to shut down the entire energy production of a storm. An interesting question one may ask is how thick the subsurface warm layer must be to be considered thick enough? In other words, what is the needed range for the subsurface parameters, such as the depth of the 26°C isotherm (i.e., D26, often used to characterize the subsurface warm layer thickness) or the upper-ocean heat content (UOHC or Q_H, i.e., the integrated heat content excess per unit area relative to the 26°C isotherm, integrated from D26 to the surface[2]) (Leipper and Volgenau 1972; Shay et al. 2000; Goni and Trinanes 2003; Pun et al. 2007; Lin et al. 2009; Mainelli et al. 2008)? Meanwhile, since the ocean's negative feedback is weaker when a storm is fast moving, will the requirements for fast- or slow-moving storms be different? It has been hinted in Part I that some faster-moving storms were observed to intensify to category 5 over a relatively shallow layer of warm water. As such, this study aims to systematically investigate and quantify the relationship between translation speed and the required subsurface parameters.

In section 2, we first examine the relationship between the observed translation speed and the upper-ocean thermal structure (UOTS) in the intensification locations of category 5 typhoons. Data from the most recent 10 yr (1997–2006) are studied because prior to 1997, very limited in situ UOTS data are available. Each typhoon's translation speed, track, and intensity data are taken from the best-track data of the Joint Typhoon Warning Center (JTWC). The in situ UOTS data are obtained from the National Oceanic and Atmospheric Administration (NOAA) Global Temperature and Salinity Profile Program (GTSPP; Keeley et al. 2003) and the Argo[3] float databases (Gould et al. 2004; Roemmich et al. 2004; Lyman et al. 2006; Willis et al. 2007). Next, the during-storm self-induced cooling negative feedback is estimated under various translation speeds and subsurface conditions using the Price–Weller–Pinkel (PWP) ocean mixed layer model (Price et al. 1986). Air–sea enthalpy fluxes are also estimated accordingly (Powell et al. 2003; Black et al. 2007; Part I; Lin et al. 2009).

In section 3, a new concept called the "affordable minimum translation speed ($U_{h\_\min}$)" is proposed. This is the minimum speed a storm has to travel to confine the self-induced cooling within a certain threshold during the intensification process to category 5, given the observed subsurface D26. Using more than 3000 Argo

[2] $Q_H = c_p \rho \Sigma_{i=1}^{n} \Delta T(x, y, z_i, t) \Delta Z$, where c_p is the heat capacity of the seawater at constant pressure (4178 J kg^{-1} °C^{-1}), ρ is the average seawater density of the upper ocean (1026 kg m^{-3}), $\Delta T(x, y, z_i, t)$ is the temperature difference between $T(z_i)$ and 26°C at depth z_i, and ΔZ is the depth increment (5 m). Here n is the total layers from surface to the depth of 26°C (D26). The total UOHC is the sum of UOHC at each depth increment (ΔZ) through the surface to the D26.

[3] In this work, all Argo profiles are prescreened to ensure data quality. As reported by Willis et al. (2007), a small subset of floats fabricated at the Woods Hole Oceanographic Institution was detected to have a cold bias. Thus, data from this batch of floats are screened out and not used in this study.

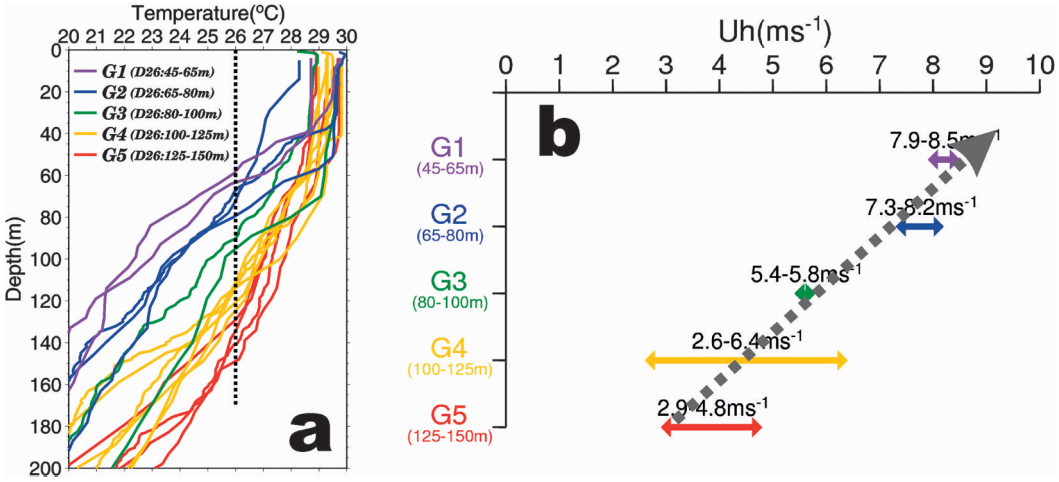

FIG. 1. (a) The searched prestorm in situ depth–temperature profiles found in the intensification locations. The profiles are sorted into five groups, according to the D26. (b) The corresponding observed translation speed for each group.

profiles (Gould et al. 2004; Roemmich et al. 2004; Lyman et al. 2006; Willis et al. 2007) to conduct a series of mixed layer model experiments, the relationship between D26 and $U_{h\_\min}$ is established. In section 4, similar relationships are established for UOHC and $U_{h\_\min}$. In section 5, issues related to future forecasts and ocean features (i.e., consolidating results with Part I), and concerns of other factors (e.g., stratification) in future research are discussed. Conclusions are given in section 6.

2. UOTS–U_h relationship observed during 1997–2006 together with the associated self-induced cooling and enthalpy flux

a. The observed UOTS–U_h relationship

Figure 1a depicts the in situ upper-ocean thermal structure profiles found in the intensification locations (from category 1 to the peak in category 5) of category 5 typhoons during the May–October typhoon season in the most recent 10 yr. Profiles are searched within 8 days prior to the passage of each storm and within a 2° radius from the best track. In total, 17 profiles from 13[4] out of the 25 category 5 typhoons are found.

As in Fig. 1a, SST values are confined within a narrow range between 28° and 30°C while large variability is found in the subsurface. Namely, the depth of the 26°C isotherm ranges from as shallow as 58 m to as deep as 150 m (i.e., ~200% difference). Based on the differences in D26, the in situ profiles can be categorized into 5 groups, from the shallowest, G1 (D26 = 45–65 m), to the deepest, G5 (D26 = 125–150 m; Fig. 1a). As summarized in Table 1, the average SST is similar among the 5 groups with values all near 29°C. In contrast, distinct differentiation can be seen in the 2 subsurface parameters that the average D26 increases from 61 in G1 to 138 m in G5 while UOHC increases from 64 to 122 kJ cm^{-2}.

Examining the observed translation speed[5] for the 5 groups (Fig. 1b), one finds that shallower layers (G1 and G2) are associated with faster translation speeds (~7.3–8.5 m s^{-1}) while over deeper waters (e.g., G4 and G5), a wider range of translation speeds is found (i.e., from the slowest 2.6 to 6.4 m s^{-1}). Also in Table 1 and Fig. 1b, one observes that with increases in D26 and UOHC from G1 to G5, the observed minimum U_h of each group decreases. These suggest that deeper warm layers (e.g., G4 and G5) allow a storm to intensify to category 5 under both slow (e.g., ~2.6 m s^{-1}) and fast (e.g., ~6.4 m s^{-1}) translation speeds (i.e., allowing a wider range of U_h for a storm to travel). However, over a shallower warm layer (e.g., G1 and G2), a storm is only allowed to travel fast (i.e., 7.3–8.5 m s^{-1}) and the range of U_h a storm is allowed to travel is also smaller (Fig. 1b).

[4] These 13 category 5 typhoons are as follows: Saomai (2006), Yagi (2006), Nabi (2005), Dianmu (2004), Chaba (2004), Maon (2004), Maemi (2003), Hagibis (2002), Fengshen (2002), Bilis (2000), Saomai (2000), Nestor (1997), and Joan (1997). For the cases of Saomai (2006), Yagi (2006), Maemi (2003), and Fengshen (2002), two profiles are found while one profile is found for the other storms. Thus, there are 17 profiles altogether.

[5] For each profile, the corresponding translation speed is calculated from the nearest point in the track.

TABLE 1. The mean (std) of the observed prestorm SST, D26, UOHC, together with the minimum, maximum, and the averaged observed translation speed for each of the five groups.

	Pre-SST (°C)	Pre-D26 (m)	Pre-UOHC (kJ cm^{-2})	Min U_h	Max U_h	Ave U_h
G1	29.3 (0.8)	61 (4)	64 (15)	7.9	8.5	8.2 (0.4)
G2	29.2 (0.8)	73 (6)	71 (31)	7.3	8.2	7.8 (0.5)
G3	28.9 (1.0)	93 (4)	96 (32)	5.4	5.8	5.6 (0.3)
G4	29.3 (0.3)	116 (5)	117 (10)	2.6	6.4	4.5 (1.4)
G5	29.3 (0.5)	138 (9)	122 (18)	2.9	4.8	4.1 (0.9)

b. Estimation of self-induced SST cooling

To further confirm the observed U_h and UOTS relationship, a mixed layer model is run for each of the five groups. As in Part I, the PWP ocean mixed layer model (Price et al. 1986) is used. The corresponding in situ profiles for each group (Fig. 1a) are used as initial profiles (Fig. 1a). For each profile, the storm-induced cooling at the inner core is estimated progressively with an increase in wind forcing from categories 1 to 5. Thus for each profile, the 10-min average maximum sustained wind, ranging from 30 to 65 m s^{-1}, at an interval of every 5 m s^{-1}, is used to drive the model. The drag coefficient used is the cyclone-wind drag coefficient (C_d) from Powell et al. (2003). Also, according to U_h, a model parameter called $\mathrm{TC}_{\text{transit-time}}$ is calculated and the model is run according to the $\mathrm{TC}_{\text{transit-time}}$ where $\mathrm{TC}_{\text{transit-time}} = D/U_h$ (D: inner core diameter of the storm). More details of the model setup can be found in Part I. Figure 2 depicts the numerical results of the group-averaged during-storm inner-core SST due to the self-induced cooling for each of the five groups according to the observed translation speeds (Fig. 1b).

One can see that for all five groups the self-induced cooling is similar and well restrained during the intensification period. Even at categories 4 and 5, the during-storm SST is still around 27°–28°C, corresponding to only around a 1°–2°C reduction from the prestorm SST of around 29°C (Figs. 2 and 3 and Table 2). Why over shallow layers (i.e., G1 and G2) can the self-induced cooling be restrained and similar to the values of those cases passing over the deeper layers (i.e., G4 and G5)?

From Fig. 4 one can see that this is due to the differences in translation speed. In Figs. 4a,b, it can be found that over shallow layers, the corresponding translation speeds are fast (i.e., 7.9–8.5 m s^{-1} for G1 and 7.3–8.2 m s^{-1} for G2, see Fig. 1b). As a result, the self-induced cooling (i.e., shaded regions in Figs. 4a,b) is comparable to the cooling over deeper layers (i.e., shaded regions in Figs. 4d,e) under slow or moderate U_h (i.e., 2.6–6.4 for G4 and 2.9–4.8 for G5, Fig. 1b). These illustrate the compensation effect of the translation speed that, even if a storm passes over a shallow warm layer, it can still be compensated by its fast translation speed to limit the self-induced cooling during the intensification process.

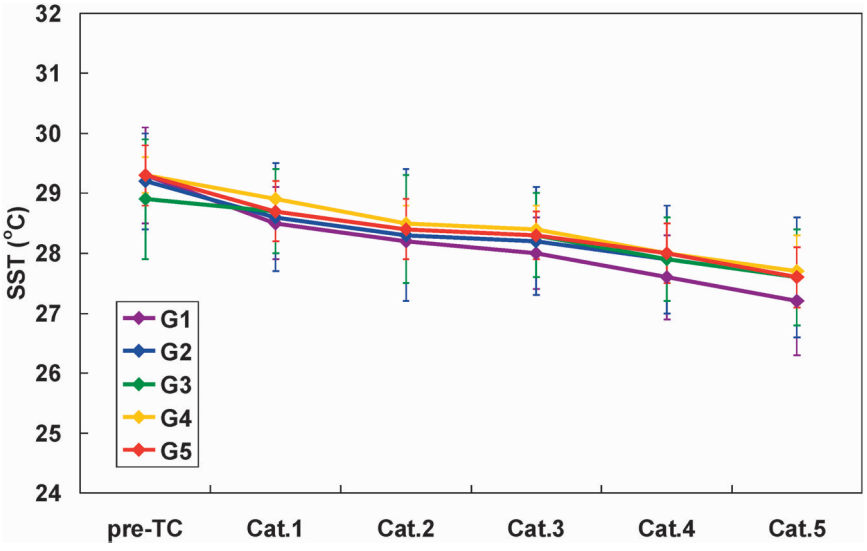

FIG. 2. Results from the PWP mixed layer numerical experiments showing the inner-core SST during the storm at various intensification periods for each of the five groups.

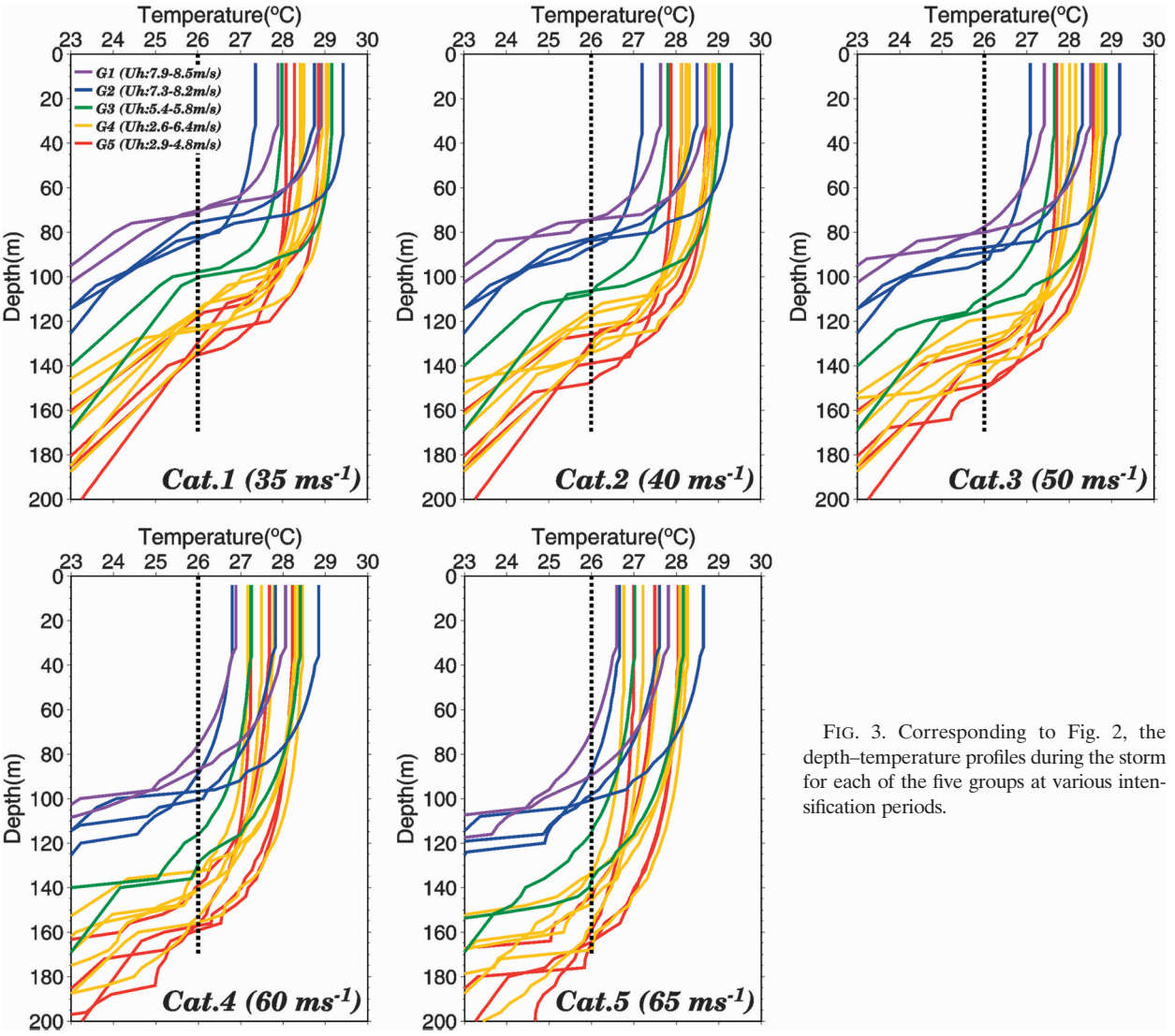

FIG. 3. Corresponding to Fig. 2, the depth–temperature profiles during the storm for each of the five groups at various intensification periods.

c. *Enthalpy flux estimation*

In order to evaluate the difference in the available air–sea enthalpy (latent + sensible heat) flux due to differences in the translation speed during the intensification process, for each group the inner-core sensible (Q_S) and latent heat fluxes (Q_L) are calculated using the bulk aerodynamic formulas (Jacob et al. 2000; Cione and Uhlhorn 2003; Powell et al. 2003; Black et al. 2007) as follows:

$$Q_S = C_H W(T_s - T_a)\rho_a C_{\mathrm{pa}}, \quad \text{and} \tag{1}$$

$$Q_L = C_E W(q_s - q_a)\rho_a L_{\mathrm{va}}, \tag{2}$$

where C_H and C_E are the sensible and latent heat exchange coefficients, respectively; W is the wind speed; T_s and T_a are SST and near surface air temperature, respectively; q_s and q_a are surface and air specific humidity, respectively; and ρ_a, C_{pa}, and L_{va} are air density, heat capacity of the air, and latent heat of vaporization, respectively. In this work, the exchange coefficients are from Black et al. (2007). Corresponding to the self-induced cooling (Fig. 4), fluxes are estimated progressively at every 5 m s^{-1} interval wind speed from categories 1 to 5, so as to cover the complete range of intensification. The near-surface atmospheric temperature and humidity data is from the 1.125° resolution data [i.e., the 40-yr European Centre for Medium-Range Weather Forecasts (ECMWF) Re-Analysis (ERA-40)]. Thus, for each typhoon case in the group, the corresponding ERA-40 data is used. Also the corresponding SST data for each typhoon case in the group is from the output of the mixed layer model (section 2b) so that the self-induced cooling

TABLE 2. The during storm self-induced SST cooling estimated from the PWP model (Price et al. 1986) for each group at various intensification periods.

	Category 1	Category 2	Category 3	Category 4	Category 5
G1	0.7 (0.2)	1.1 (0)	1.2 (0.1)	1.7 (0.1)	2.1 (0.1)
G2	0.6 (0.3)	0.9 (0.4)	1.0 (0.4)	1.3 (0.5)	1.6 (0.5)
G3	0.2 (0.2)	0.5 (0.1)	0.6 (0.1)	1.0 (0.2)	1.3 (0.2)
G4	0.4 (0.2)	0.8 (0.3)	0.9 (0.3)	1.3 (0.4)	1.6 (0.5)
G5	0.6 (0.2)	0.9 (0.1)	1.0 (0.1)	1.3 (0.2)	1.6 (0.2)

effect during the intensification process can be incorporated. As in Fig. 4, the during-storm available enthalpy fluxes for each group under various translation speeds (i.e., $U_h = 1, 2, 3, \ldots, 10$ m s^{-1}) are estimated.

Figure 5 depicts the averaged available enthalpy flux at inner core for each group. It can be seen that the flux condition is consistent with the self-induced cooling results that even over shallow waters like G1 and G2, there can still be sufficient flux available during intensification, as long as the translation speed is fast enough. One can see that with the observed U_h of about 7.9–8.5 m s^{-1} for G1 (shaded region in Fig. 5a) and U_h of 7.3–8.2 m s^{-1} for G2 (shaded region in Fig. 5b), the available flux is comparable to the available flux over deeper waters under moderate or slow speeds (e.g., shaded regions in Figs. 5d,e where $U_h = 2.6$–6.4 m s^{-1} for 5d and $U_h = 2.9$–4.8 m s^{-1} for 5e). Typically, at categories 1 and 2 the enthalpy flux is around 500–700 W m^{-2}, at category 3 it is ~800–900 W m^{-2}, and at categories 4 and 5 it is around 1000–1500 W m^{-2}. It can also be seen in Figs. 5a,b that if passing a shallow warm layer at a moderate or slow speed (e.g., $U_h = 1$–4 m s^{-1}), it is not possible to intensify to category 5 because the available enthalpy flux is around zero before reaching category 5.

3. Concept of the affordable minimum translation speed (U_{h_min}) and the minimum D26 (D26$_{_min}$)

From the above discussion, one can see that a shallow warm layer allows a storm to intensify to category 5 only under a fast translation speed. Over a deeper warm layer, a storm is allowed to travel much slower and can intensify to category 5 under both fast and slow translation speeds. As such, it will be useful to identify a critical minimum translation speed for each specific warm layer. Thus, in this work, a new concept, affordable

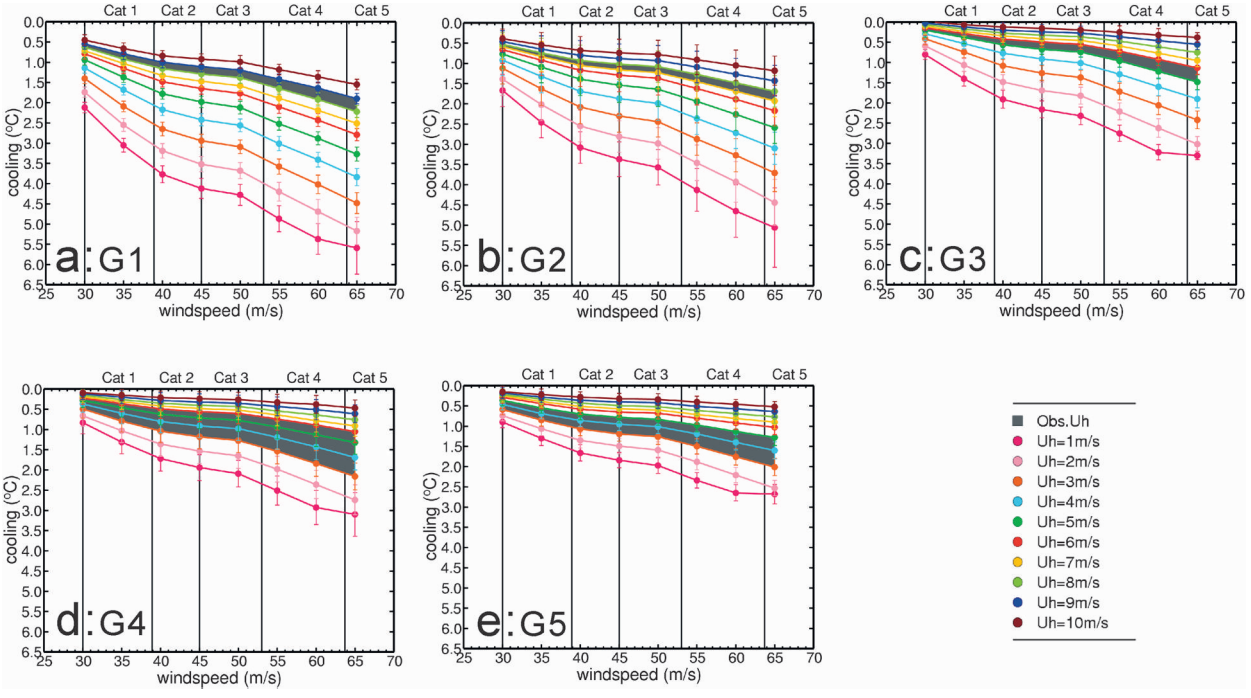

FIG. 4. The averaged self-induced ocean cooling negative feedback estimated using the PWP model for each of the five groups under progressively increasing wind forcing (interval every 5 m s^{-1}) from categories 1 to 5. For each group, self-induced cooling is estimated at various translation speeds (i.e., $U_h = 1, 2, 3, \ldots, 10$ m s^{-1}) and the observed range of U_h is shaded in dark gray.

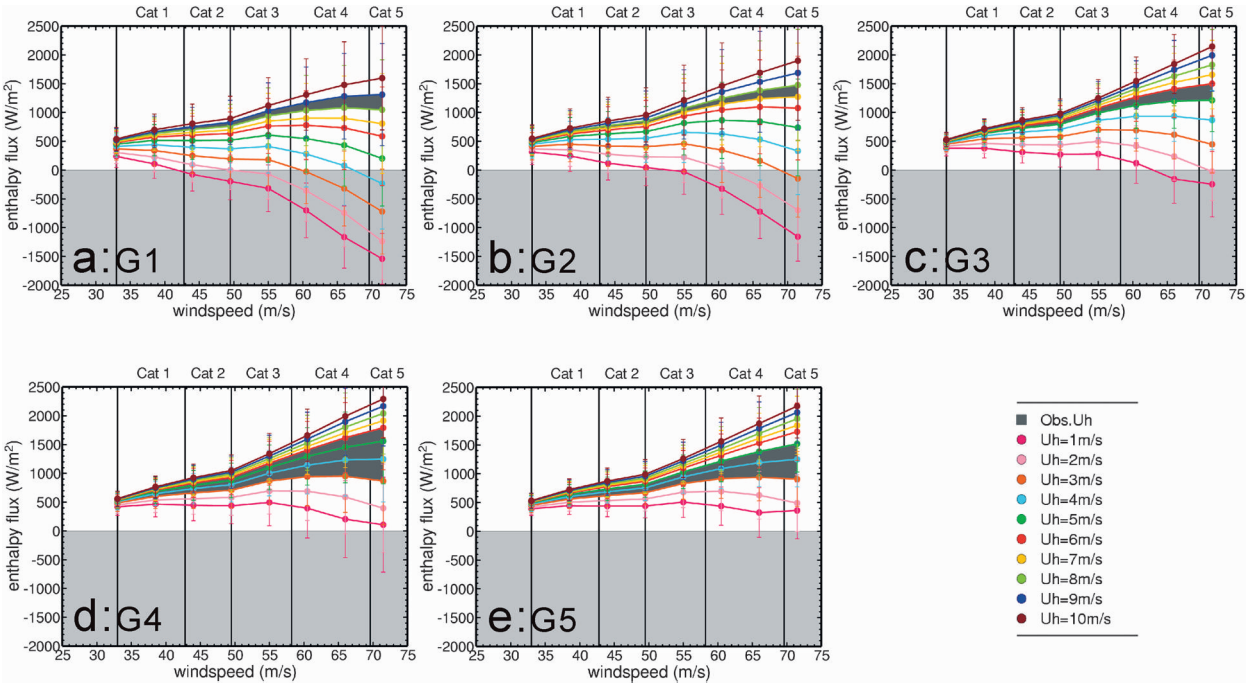

FIG. 5. As in Fig. 4, the estimated averaged enthalpy flux for each of the 5 groups during the intensification period from categories 1 to 5. For each group, enthalpy flux is estimated at various translation speeds (i.e., U_h = 1, 2, 3, . . . , 10 m s^{-1}) and the observed range of U_h is shaded in dark grey. Also, the region of enthalpy flux below 0 is shaded in light gray, indicating an unsuitable condition for intensification.

minimum translation speed, U_{h_min}, is proposed. This is the critical minimum speed a storm has to travel during its intensification process to category 5, so that the self-induced SST cooling negative feedback can be restrained within a chosen threshold, given an upper-ocean thermal profile. As in Fig. 4 and Table 2, 2.2°C is the maximum self-induced cooling found during the intensification process among all the category 5 typhoons over the past 10 yr; thus, a threshold of 2.2°C is used.

This concept can be explained using examples in Fig. 6. Given 2 profiles of similar SST values (both ~29.7°C), but having different warm layer thicknesses, one over a shallow D26 of 67 m (profile 1) and the other over a deep D26 of 134 m (profile 2), the self-induced cooling results are very different (Fig. 6b for profile 1 and Fig. 6c for profile 2). As in Fig. 6b, over the shallow warm layer, a storm has to travel at a speed 8 m s^{-1} to prevent the self-induced SST cooling from falling below the threshold (i.e., to be confined within the light gray shaded region). However, if over the deep warm layer, a storm can afford to travel more slowly, as at 4 m s^{-1}, to keep the self-induced cooling restrained (i.e., within the light gray shaded region in Fig. 6c). Therefore for profile 1, U_{h_min} is 8 m s^{-1} while for profile 2, U_{h_min} is reduced to 4 m s^{-1}.

Applying this concept and running the mixed layer model (Price et al. 1986) on profiles in Fig. 1a under various U_h (i.e., 1, 2, ... , 10 m s^{-1}), a respective U_{h_min} for each profile is identified. As depicted in Fig. 7a, a clear negative dependence between D26 and U_{h_min} is found, with a correlation coefficient R of −0.86. To further confirm this relationship, the 17 profiles in Fig. 1a are too few in number and more profiles are needed. Therefore, we search from the Argo database (Gould et al. 2004; Roemmich et al. 2004) all available in situ profiles found in the region between 10°–26°N and 120°–170°E (boxed region in Fig. 8a) because this is the observed intensification domain for category 5 typhoons, as identified in Part I. As Argo floats became available in 2000 (Gould et al. 2004), all typhoon season (May–October) profiles from 2000 to 2006 are searched. Also from Fig. la and Table l, 28°C is the minimum observed value for SST in the intensification locations of category 5 typhoons, profiles of 28°C are used. In total, 3326 profiles are identified, as depicted in Fig. 8b (gray profiles). It can be seen in Fig. 8a that though these profiles may not be the ones found directly along the track of historical category 5 typhoons (i.e., the profiles in Fig. 1a), they are still the valid candidate profiles for possible intensification to category 5 because they are from the same intensification region during the typhoon season. It can be observed in Fig. 8b that the depth–temperature distribution of these profiles is similar and consistent to the ones found along the track.

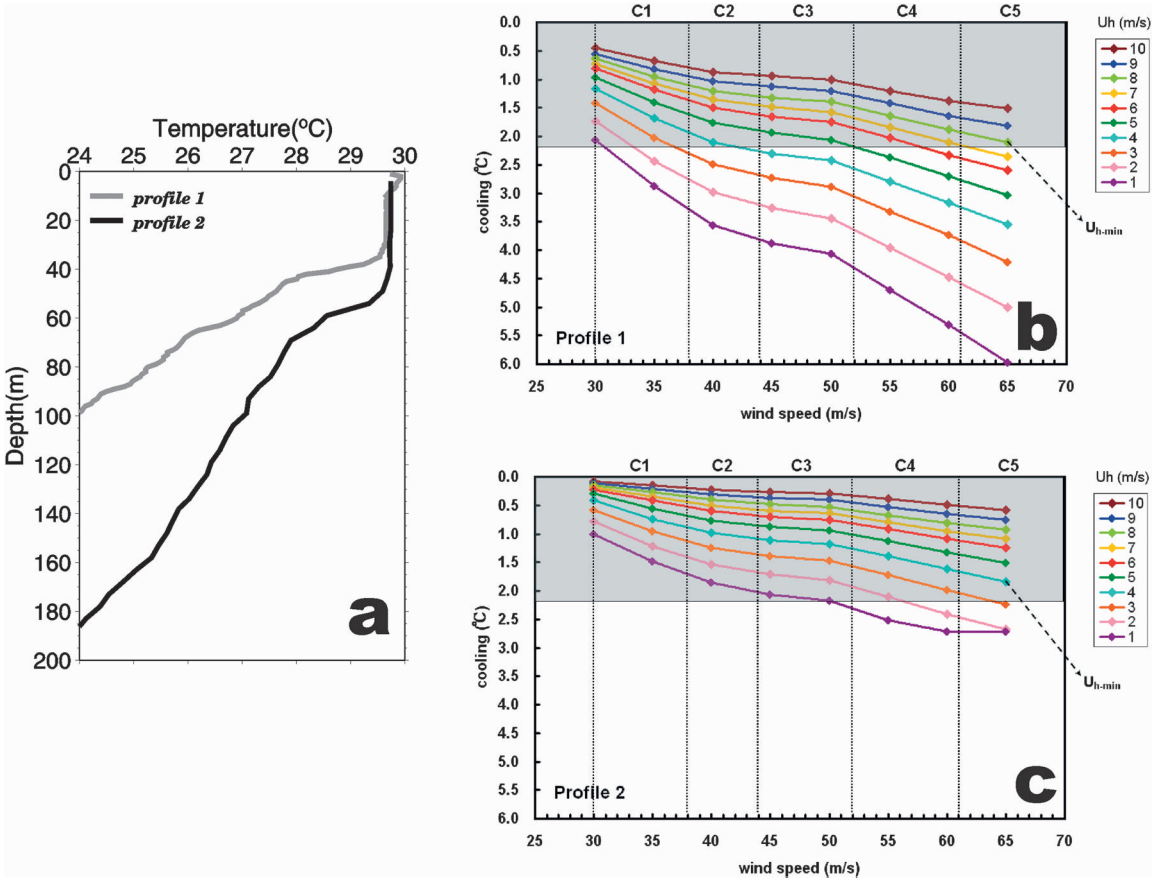

FIG. 6. (a) Two example profiles showing similar SSTs (both ~29.7°C) but of different warm layer thickness, one over shallow D26 of 67 m (profile 1) and the other over deep D26 of 134 m (profile 2). (b) The estimated self-induced ocean cooling at various translation speeds for profile 1 with $U_{h\_\min}$ indicated. Region of cooling confined within the 2.2°C threshold is shaded in light gray, indicating possible condition for intensification. (c) As in (b), but for profile 2.

Running the mixed layer model on these >3000 profiles, $U_{h\_\min}$ for each profile is identified. As depicted in Fig. 7b, a similar negative dependence between D26 and $U_{h\_\min}$ is found, with a correlation coefficient R of −0.87. Applying the least squares fit over these 3326 D26–$U_{h\_\min}$ pairs, a first-order relationship between D26 and $U_{h\_\min}$ is obtained as

$$U_{h\_\min} = -0.065 \times \mathrm{D26} + 11.1. \quad (3)$$

This provides a simple way to quantify the minimum translation speed required during intensification to category 5, given D26. In addition, since Fig. 7b depicts a linear dependence, it can also be used to estimate the required minimum D26 (i.e., $\mathrm{D26}_{\_\min}$), if given U_h (Fig. 7c) as

$$\mathrm{D26}_{\_\min} = -11.7 \times U_h + 155. \quad (4)$$

From above, it can be seen that the thickness of the subsurface warm layer that is required for intensification to category 5 is a function sensitive to translation speed and that the requirements between fast- and slow-moving storms are different.

Testing the validity of the relationships in Eqs. (3) and (4) using the actual 10-yr observations in section 2a, one can see that this new concept is supported by the observations. As in Table 1, the averaged observed D26 for groups 1–5 are 61, 73, 93, 116, and 138 m, respectively. Using Eq. (3), one can calculate the corresponding $U_{h\_\min}$ = 2, 3.5, 5, 6.3, and 7 m s^{-1}. Therefore, one can see that if a storm is to intensify to category 5 over the shallowest G1 waters, it needs to traverse at a speed 7 m s^{-1}. Examining the observed U_h range for G1, one sees that it fell between 7.9 and 8.5 m s^{-1} (Table 1 and Fig. 1b), that is, in good agreement with the estimated $U_{h\_\min}$ of 7 m s^{-1}. Checking the other four groups, similar agreements are also found. For example over the G5 waters, the observed range of U_h is 2.9–4.8 m s^{-1} and the $U_{h\_\min}$ = 2 m s^{-1} (Table 1 and Fig. 1b).

Next, Eq. (4) is tested. As in Table 1, the observed averaged U_h for G1 to G5 are 8.2, 7.8, 5.6, 4.5, and 4.1 m s^{-1}. Using Eq. (4), the corresponding $\mathrm{D26}_{\_\min}$ is

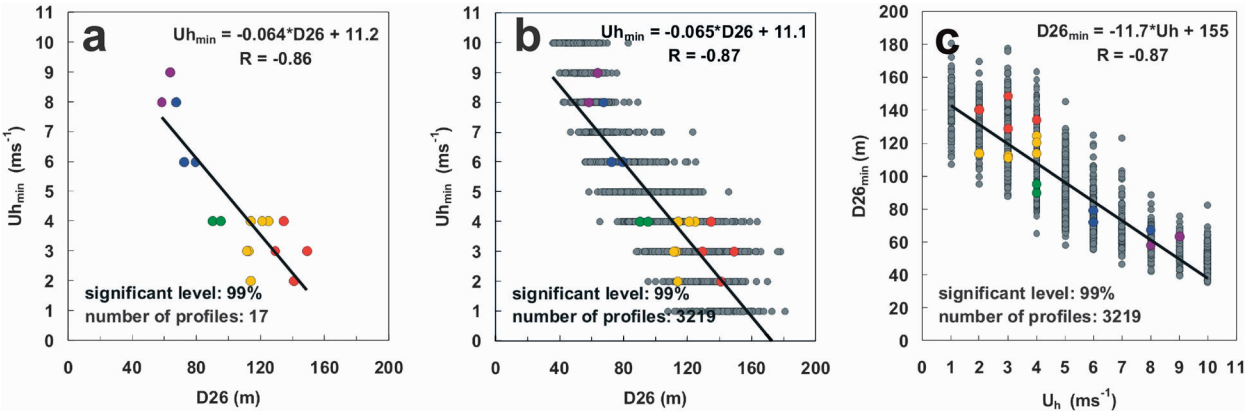

FIG. 7. (a) The D26–$U_{h\_\min}$ relationship obtained from the 17 profiles in Fig. 1a. (b) As in (a), but obtained from the 3326 profiles in Fig. 8b with the 17 pairs in (a) overlaid (color scheme for each group see Fig. 1a). (c) As in (b), but for the U_h–D26$_{_\min}$ relationship.

estimated to be 59, 64, 89, 102, and 107 m, respectively. Examining the observed averaged D26, indeed they satisfy this required minimum and the corresponding observed averaged D26 are 61, 73, 93, 116, and 138 m (i.e., D26$_{_\min}$). Therefore, Eqs. (3) and (4) can be used to quantify the minimum subsurface requirements for intensification to category 5. If given the observed translation speed, one can estimate the required minimum D26 using Eq. (4). Conversely, if given the observed D26, Eq. (3) can be used to estimate the required minimum U_h.

4. Affordable minimum translation speed and the minimum upper-ocean heat content

Besides D26, another subsurface parameter of interest is the upper-ocean heat content (Leipper and Volgenau 1972; Shay et al. 2000; Goni and Trinanes 2003; Pun et al. 2007; Part I; Lin et al. 2009). Using the more than 3000 in situ Argo profiles in Fig. 8b, UOHC is calculated. First, UOHC is compared with D26. As shown in Fig. 9a, UOHC is highly correlated with D26, with $R = 0.86$. Examining the UOHC for each profile with the corresponding $U_{h\_\min}$, similar dependence ($R = -0.71$) is found as D26 and $U_{h\_\min}$. Therefore, similar to results presented in section 3, simple linear relationships (Figs. 9b,c) are obtained as

$$U_{h\_\min} = -0.05 \times \text{UOHC} + 9.4, \quad \text{and} \qquad (5)$$

$$\text{UOHC}_{\_\min} = -10.1 \times U_h + 142. \qquad (6)$$

Also, it should be clarified that the "lower UOHC" refers to a shallow subsurface warm layer situation and not a SST reduction situation. UOHC is integrated from surface (SST) down to D26, therefore besides the shallow subsurface warm layer, low SST can also cause low

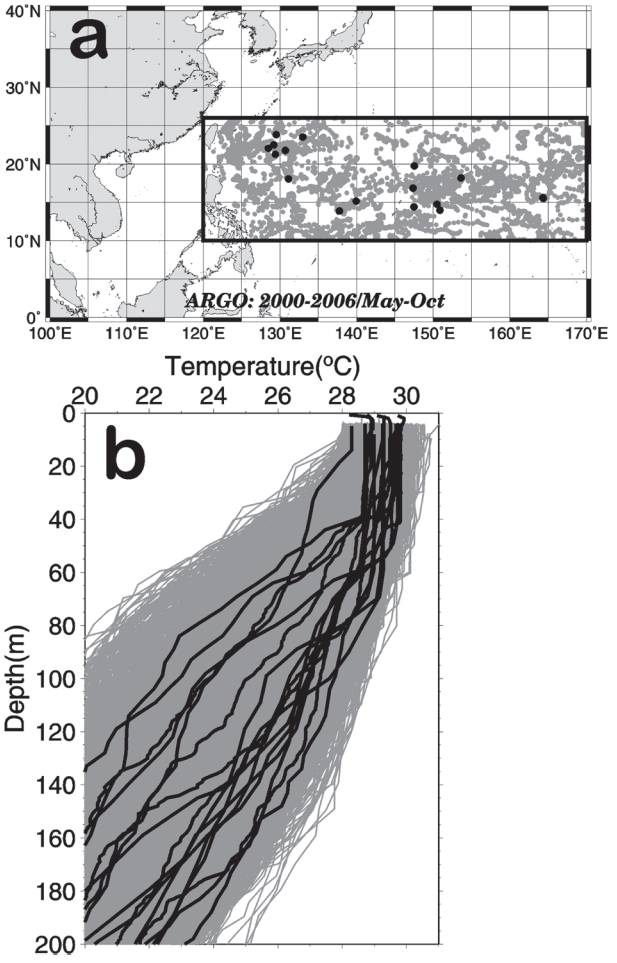

FIG. 8. (a) Locations (in gray) of the 3326 Argo in situ profiles searched from the region between 10°–26°N and 120°–170°E during the May–October typhoon season between 2000 and 2006. The location of the profiles in Fig. 1a are overlaid and depicted in black. (b) The depth–temperature distribution of the 3326 profiles (in gray) with the profiles in Fig. 1a overlaid (in black).

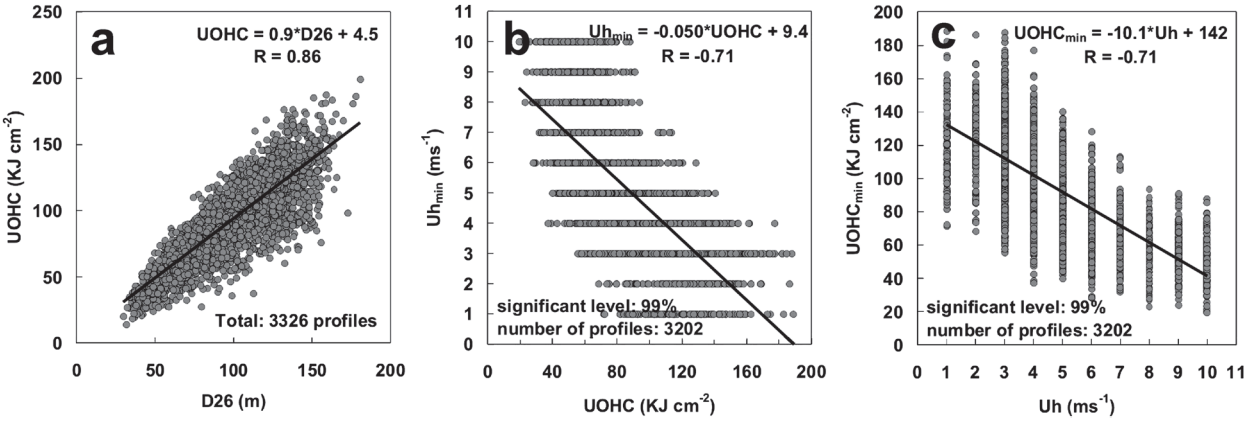

FIG. 9. (a) The dependence between D26 and UOHC. (b) The UOHC–$U_{h\_\min}$ relationship obtained from the 3326 profiles in Fig. 8b. (c) The U_h–UOHC$_{_\min}$ relationship for the 3326 profiles in Fig. 8b.

UOHC. However, from Figs. 1a and 8b and Table 1, the prestorm SSTs in this work are all ≥28°C (i.e., warm SST is a prerequisite; based on 10-yr in situ observations in section 2) to be considered before meeting the subsurface condition (i.e., D26 and UOHC). As such, the lower UOHC in the context of this study refers to a shallow subsurface warm layer, not a reduction in SST.

5. Discussion

a. Suggestion for future forecast reference

In recent years, there has been an increasing demand to incorporate subsurface information like D26 and UOHC as forecast indicators (Shay et al. 2000; Goni and Trinanes 2003; Lin et al. 2005, 2009; Part I; Pun et al. 2007). From the results of this work, one can see that since the subsurface requirements for fast- and slow-moving storms are different, it will be more accurate to consider the subsurface parameters with respect to the translation speed. For example, convenient lookup tables (LUTs) can be generated from Figs. 7c and 9c so that given a storm's observed or predicted U_h, the required minimum D26 and UOHC can be used to test whether the actual subsurface warm layer is thick enough to satisfy the minimum requirement. As in Tables 3 and 4, given U_h = 1–3, 4–6, and 7–9 m s^{-1}, the corresponding average D26$_{_\min}$ (UOHC$_{_\min}$) is about 124–144 m (116–122 kJ cm^{-2}), 76–107 m (75–104 kJ cm^{-2}), and 56–68 m (56–66 kJ cm^{-2}), respectively. Also in Tables 3 and 4, standard deviations are given, so as to provide reference to account for the spreading observed in Figs. 7c and 9c.

b. Interrelationship with ocean features

In Part I, the role that ocean features [i.e., the positive or negative sea surface height anomaly (SSHA) features detected from satellite altimetry] play in the intensification of category 5 typhoons is discussed. Consolidating the results found in this work and Part I, the interrelationship between the translation speed, features encountered, and subsurface warm layer in a category 5 typhoon's intensification is discussed as follows. Basically it is a matter of meeting the minimum subsurface requirement established in this work and three factors are involved: translation speed, the background climatological UOTS, and the actual in situ UOTS modulated by the presence of the ocean features.[6] If the observed translation speed is given, the background climatological warm layer is too shallow to meet the minimum requirement, then encountering the positive SSHA feature is needed so that the warm layer can be deepened from the background to meet the minimum.

Using the $U_{h\_\min}$ concept in this work, Fig. 10 can be used as a reference in guiding the interpretation of feature encountering. Figure 10 depicts $U_{h\_\min}$ (annotated in stars) for various background D26 [based on Eq. (3)]. If the actual $U_h < U_{h\_\min}$ (i.e., fall within the range between 0 and $U_{h\_\min}$, dashed arrows) then encountering a positive SSHA feature is necessary because the storm is not traveling fast enough. On the other hand, if the actual $U_h \geqq U_{h\_\min}$ (solid arrows), then encountering the positive SSHA feature is not necessary. Also from Fig. 10, the applicable ranges for the three subregions [i.e., the south eddy zone (SEZ),

[6] As explained in Part I, features detected from satellite altimetry represents the deviation of the current in situ UOTS from the background climatological UOTS. Therefore, there can be three possible scenarios: 1) positive SSHA feature (i.e., deepening of the subsurface warm layer from the climatological background), 2) no SSHA feature (i.e., no deepening and shoaling, the actual subsurface warm layer is similar to the background), or 3) negative SSHA feature (i.e., shoaling of the subsurface warm layer from the background climatology).

TABLE 3. Lookup table of the required minimum D26 (i.e., $D26_{\_min}$) under various translation speeds based on Fig. 7c.

U_h (m s^{-1})	1	2	3	4	5	6	7	8	9	10
Mean D26 (m)	144	134	124	107	90	76	68	61	56	50
Std dev	13	13	15	15	14	11	11	8	7	7
Mean ± std dev	131–157	121–147	109–139	92–122	76–104	65–87	57–79	53–69	49–63	43–57

Kuroshio, and the central gyre] in the western North Pacific identified in Part I are depicted. It can be clearly seen that the shallower the background (e.g., the SEZ), the larger the corresponding U_{h_min}, the more encountering of positive SSHA features (i.e., over wider range of U_h) is needed, and vice versa.

c. Issues on changing the threshold

In this study, because 2.2°C is the maximum self-induced cooling found during the intensification to category-5 in the past 10 yr (Table 2), it is used as the threshold value to obtain the minimum translation speed (sections 3 and 4). If one replaces the threshold using the mean self-induced cooling value of around 1.6°C (i.e., last column in Table 2) instead of 2.2°C and redoes the mixed layer experiments, then the new D26–U_h pairs and the regression relationship would provide the mean translation speed (U_{h_mean}) instead of the minimum. In other words, given D26 or UOHC, U_{h_min} is the minimum speed a storm has to travel to keep the self-induced cooling below the maximum cooling of 2.2°C while U_{h_mean} would be the mean speed a storm travels to keep the cooling at the mean value of around 1.6°C. As can be seen in Fig. 11, the new regression relationship is given as

$$U_{h\_mean} = -0.06 \times \mathrm{D26} + 12.1. \quad (7)$$

By comparing the new regression relationship [black solid curve in Fig. 11a, i.e., Eq. (7)] with the relationship for the U_{h_min} [brown solid curve in Fig. 11a or black curve in Fig. 7b, i.e., (3)], one can see that given the same D26, $U_{h\_mean} > U_{h\_min}$. By overlaying the actual observed D26 and U_h pairs for the category 5 typhoons in the past 10 yr (i.e., from section 2a), one can see that this mean relationship matches well the actual observations and the regression relationship derived from the actual D26–U_h pairs [i.e., the black dash regression line in Fig. 11a, $U_{h\_obs} = -0.055 \times D26_{\_obs} + 11.3$, Eq. (8)] is almost identical to Eq. (7). Similarly as in Fig. 11b, if given U_h, the corresponding $D26_{\_mean} > D26_{\_min}$.

d. Issues on other factors

Though in this work the focus is on the role of the translation speed, it does not imply that other factors are not important. For example, issues related to typhoon size, ocean's horizontal advection, upwelling, and stratification are also important factors consider in the future. For example when considering the thermocline stability below the ocean mixed layer, the Brunt–Väisälä frequency N^2 can be calculated from the Argo profiles. With this extra information, one can further subdivide the $D26_{\_min}$–U_h pairs (i.e., Fig. 7c) into two groups, one under the small regular N^2 condition (here $\leqq 4\times10^{-4}\mathrm{s}^{-2}$ is used as the criterion, Fig. 12a) while the other under the large N^2 condition (Fig. 12b). Thus, regression relationships can be obtained separately for these two subgroups. As can be seen in Fig. 12b, under the large N^2 (i.e., more stratified) condition, it does not need as deep the subsurface warm layer to intensify to category 5; for example, if given $U_h = 5$ m s^{-1}, the corresponding $D26_{\_min}$ is ~82 m under the large N^2 condition (Fig. 12b) and ~99 m under the small regular N^2 condition. This is reasonable since large N^2 is unfavorable for mixing and thus inhibits the self-induced cooling negative feedback. As such, if the N^2 is large, the subsurface warm layer required for intensification to category 5 is not as deep as compared to the small regular N^2 condition.

Finally, it should also be mentioned that the ocean's condition (including SST and subsurface) is a necessary but not a sufficient condition for intensification and the focus of this work is to explore the borderline of the ocean's necessary subsurface condition with respect to the translation speed for category 5 typhoons. Certainly it is not possible to reach category 5 without meeting all other favorable atmospheric and storm structure

TABLE 4. Lookup table of the required minimum UOHC (i.e., $UOHC_{\_min}$) under various translation speeds based on Fig. 9c.

U_h (m s^{-1})	1	2	3	4	5	6	7	8	9	10
Mean UOHC (kJ cm^{-2})	122	122	116	104	89	75	66	58	56	50
Std dev	25	23	24	22	20	18	17	15	14	14
Mean ± std dev	97–147	99–145	92–140	82–126	69–109	57–93	49–83	43–73	42–70	36–64

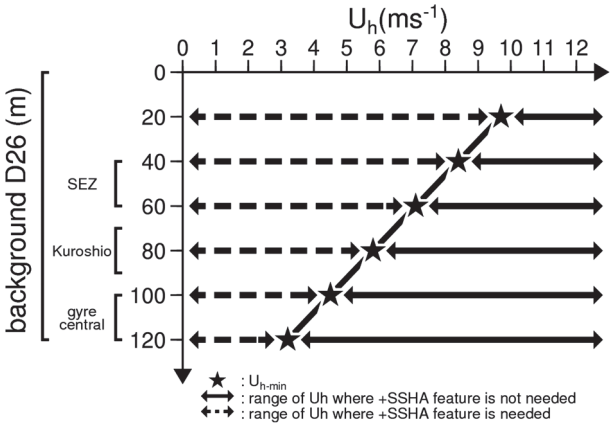

FIG. 10. The corresponding U_{h_min} (annotated in stars) for various background D26 [based on Eq. (3)]. Also, the range of U_h where encountering the positive SSHA feature is needed is depicted in dashed arrows, while the range of U_h where encountering the positive SSHA feature is not needed is depicted in solid arrows. The applicable range of the background D26 for the three subregions (i.e., SEZ, Kuroshio, and the gyre central) in the western North Pacific, as identified in Part I, is also depicted for reference.

conditions (e.g., Merrill 1988; Frank and Ritchie 2001; Wang and Wu 2003; Emanuel et al. 2004; Montgomery et al. 2006; Houze et al. 2007; Mainelli et al. 2008).

6. Conclusions

Category 5 cyclones are the most intense cyclones on earth. For a long time it has been known that in addition to warm SST, a sufficiently thick layer of subsurface warm water is required as a necessary precondition for reaching such a high intensity (e.g., Leipper and Volgenau 1972; Gray 1979). However, because of the lack of in situ observations it has been difficult to quantify how thick a subsurface warm layer is considered as thick enough. With the advancement in in situ ocean observations like the deployment of Argo floats (Roemmich et al. 2004; Trenberth 2006), it is now possible to take a fresh look at the situation using new observations. Based on 10 yr of data, it is found that SST is typically around 29°C. However, the subsurface condition depends strongly on cyclone's translation speed.

It is observed that faster-moving typhoons of $U_h \sim$ 7–8 m s^{-1} can afford to intensify to category 5 over a shallow subsurface warm layer characterized by D26 $\sim$ 60–70 m and UOHC $\sim$ 65–70 kJ cm^{-2} while slow-moving typhoons need much deeper subsurface layers; for example, D26 $\sim$ 115–140 m and UOHC $\sim$ 115–125 kJ cm^{-2} are needed for traveling at $U_h \sim$ 2–3 m s^{-1}. Ocean mixed layer numerical experiments and air–sea enthalpy flux estimations support the above observations that though over relatively shallow layer, there is still sufficient flux for intensification since the negative feedback from cyclone's self-induced cooling (Price 1981; Emanuel 1999) can still be effectively restrained under fast translation speed. On the contrary, as the negative feedback is much enhanced when a storm is slow moving (Price 1981; Lin et al. 2003a,b), a much deeper subsurface warm layer is required for slow-moving typhoons.

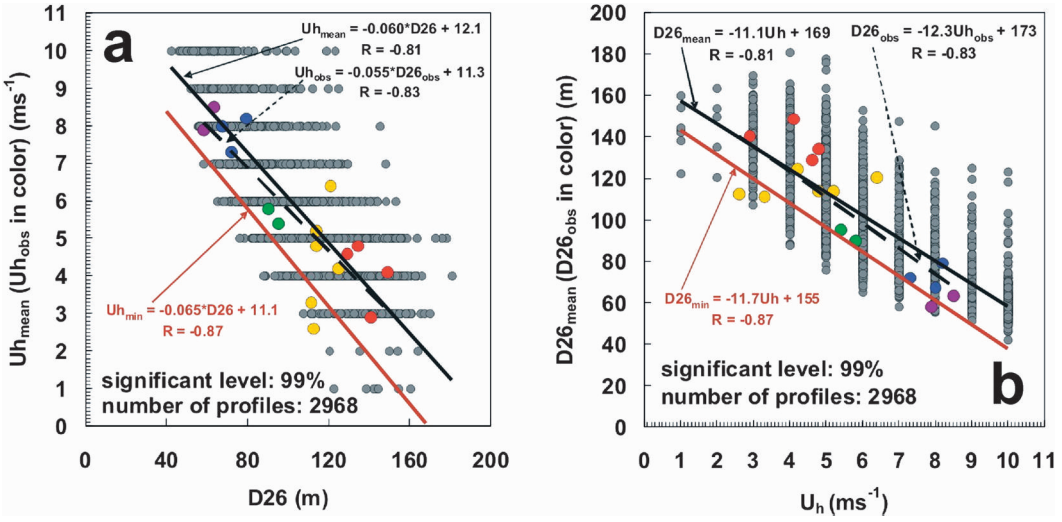

FIG. 11. (a) The D26–U_{h_mean} pairs obtained using the mean self-induced cooling of 1.6°C with the regression relationship depicted with a black solid line. The regression relationship from Fig. 7b is depicted with a brown solid line for reference. The actual observed 17 U_h–D26 pairs in the past 10 yr are depicted in color (color scheme for each group see Fig. 1a) with the regression relationship derived using these actual observations in the black dashed line. (b) As in (a), but for the U_h–D26$_{min}$ pairs.

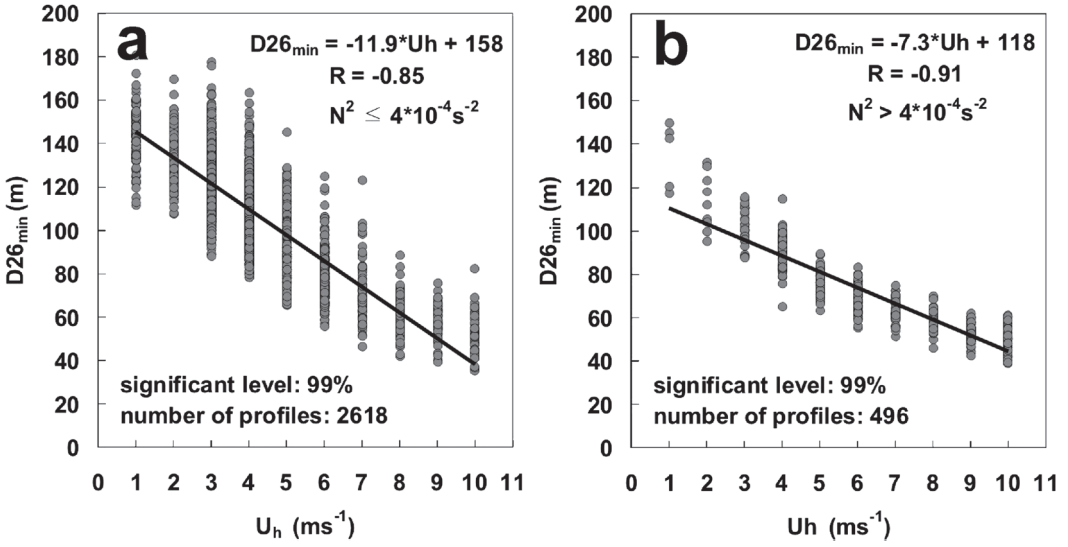

FIG. 12. (a) The U_h–D26$_{_min}$ relationship under the small regular N^2 condition (i.e., $N^2 \leqq 4 \times 10^{-4}\ s^{-2}$). (b) As in (a), but under the large N^2 (i.e., $N^2 > 4 \times 10^{-4}\ s^{-2}$) condition.

Given the above observed strong dependence between translation speed and the subsurface parameters, in this work, a new concept named the affordable minimum translation speed (U_{h_min}) is proposed. This is the minimum speed a storm has to travel to keep the self-induced cooling negative feedback restrained within a certain threshold during the intensification process to category 5, given the observed D26 or UOHC. Using more than 3000 Argo profiles (Gould et al. 2004; Roemmich et al. 2004), a series of mixed layer model experiments are conducted to quantify the relationships between D26 (UOHC) and U_{h_min}. Linear relationships with correlation coefficients $R = -0.87$ (-0.71) are obtained as $U_{h\_min} = -0.065 \times \text{D26} + 11.1$, and $U_{h\_min} = -0.05 \times \text{UOHC} + 9.4$, respectively. As both relationships are linear, they can in turn be used to estimate the minimum required D26 and UOHC, given the observed U_h (i.e., $\text{D26}_{\_min} = -11.7 \times U_h + 155$ and $\text{UOHC}_{\_min} = -10.1 \times U_h + 142$. Typically, for U_h = 1–3, 4–6, and 7–9 m s^{-1}, the corresponding average D26$_{_min}$ (UOHC$_{_min}$) is about 124–144 m (116–122 kJ cm^{-2}), 76–107 m (75–104 kJ cm^{-2}), and 56–68 m (56–66 kJ cm^{-2}), respectively.

Finally, the findings in this work are consolidated with the results in Part I and the relationship with ocean features and suggestions for future forecast reference are made.

Acknowledgments. The authors wish to thank Prof. Dong-Ping Wang for providing the mixed layer model, to Mr. Chi Hong Chen for data processing, to the reviewers for their valuable comments. Thanks also to the Joint Typhoon Warning Center, Remote Sensing System, NASA Jet Propulsion Laboratory, NOAA/GTSPP, and the Argo float teams for data provision. This work is supported by the National Science Council, Taiwan through Grants NSC97-2111-M-002-014-MY3, NSC 95-2611-M-002-024-MY3, and the joint program between the Taiwan National Science Council's Integrated Typhoon-Ocean Program (ITOP) and the U.S. Office of Naval Research's Typhoon DRI Program.

REFERENCES

Black, P. G., and Coauthors, 2007: Air–sea exchange in hurricanes: Synthesis of observations from the Coupled Boundary Layer Air–Sea Transfer Experiment. *Bull. Amer. Meteor. Soc.,* **88,** 357–374.

Cione, J. J., and E. W. Uhlhorn, 2003: Sea surface temperature variability in hurricanes: Implications with respect to intensity change. *Mon. Wea. Rev.,* **131,** 1783–1796.

Emanuel, K. A., 1995: Sensitivity of tropical cyclones to surface exchange coefficients and a revised steady-state model incorporating eye dynamics. *J. Atmos. Sci.,* **52,** 3969–3976.

——, 1997: Some aspects of hurricane inner-core dynamics and energetics. *J. Atmos. Sci.,* **54,** 1014–1026.

——, 1999: Thermodynamic control of hurricane intensity. *Nature,* **401,** 665–669.

——, 2005: Increasing destructiveness of tropical cyclones over the past 30 years. *Nature,* **436,** 686–688.

——, C. DesAutels, C. Holloway, and R. Korty, 2004: Environmental control of tropical cyclone intensity. *J. Atmos. Sci.,* **61,** 843–858.

Frank, W. M., and E. A. Ritchie, 2001: Effects of vertical wind shear on the intensity and structure of numerically simulated hurricanes. *Mon. Wea. Rev.,* **129,** 2249–2269.

Gallacher, P. C., R. Rotunno, and K. A. Emanuel, 1989: Tropical cyclogenesis in a coupled ocean–atmosphere model. Preprints, *18th Conf. on Hurricanes and Tropical Meteorology,* San Diego, CA, Amer. Meteor. Soc., 121–122.

Goni, G. J., and J. A. Trinanes, 2003: Ocean thermal structure monitoring could aid in the intensity forecast of tropical cyclones. *Eos, Trans. Amer. Geophys. Union,* **84,** 573–580.

Gould, J., and Coauthors, 2004: Argo profiling floats bring new era of in situ ocean observations. *Eos, Trans. Amer. Geophys. Union,* **85,** 179, 190–191.

Gray, W. M., 1977: Tropical cyclone genesis in the western North Pacific. *J. Meteor. Soc. Japan,* **55,** 465–482.

——, 1979: Hurricanes: Their formation, structure and likely role in the tropical circulation. *Meteorology over the Tropical Oceans,* D. B. Shaw, Ed., Royal Meteorological Society, 155–218

Holliday, C. R., and A. H. Thompson, 1979: Climatological characteristics of rapidly intensifying typhoons. *Mon. Wea. Rev.,* **107,** 1022–1034.

Houze, R. A., Jr., S. S. Chen, B. F. Smull, W. C. Lee, and M. M. Bell, 2007: Hurricane intensity and eyewall replacement. *Science,* **315,** 1235–1239.

Jacob, S. D., L. K. Shay, A. J. Mariano, and P. G. Black, 2000: The 3D oceanic mixed layer response to hurricane Gilbert. *J. Phys. Oceanogr.,* **30,** 1407–1429.

Johnson, G. C., S. Levitus, J. M. Lyman, C. Schmid, and J. Willis, 2006: Ocean heat content variability. NOAA annual report on the state of the ocean and the ocean observing system for climate, NOAA, 74–84.

Keeley, B., C. Sun, and L. P. Villeon, 2003: Global Temperature and Salinity Profile Program annual report. NOAA/National Oceanographic Data Center, Silver Spring, MD, 32 pp.

Leipper, D., and D. Volgenau, 1972: Hurricane heat potential of the Gulf of Mexico. *J. Phys. Oceanogr.,* **2,** 218–224.

Lin, I. I., W. T. Liu, C. C. Wu, J. C. H. Chiang, and C. H. Sui, 2003a: Satellite observations of modulation of surface winds by typhoon-induced upper ocean cooling. *Geophys. Res. Lett.,* **30,** 1131, doi:10.1029/2002GL015674.

——, and Coauthors, 2003b: New evidence for enhanced ocean primary production triggered by tropical cyclone. *Geophys. Res. Lett.,* **30,** 1718, doi:10.1029/2003GL017141.

——, C. C. Wu, K. A. Emanuel, I. H. Lee, C. R. Wu, and I. F. Pun, 2005: The interaction of Supertyphoon Maemi (2003) with a warm ocean eddy. *Mon. Wea. Rev.,* **133,** 2635–2649.

——, ——, I. F. Pun, and D. S. Ko, 2008: Upper-ocean thermal structure and the western North Pacific category-5 typhoons. Part I: Ocean features and category-5 typhoon's intensification. *Mon. Wea. Rev.,* **136,** 3288–3306.

——, C. H. Chen, I. F. Pun, W. T. Liu, and C. C. Wu, 2009: Warm ocean anomaly, air sea fluxes, and the rapid intensification of tropical cyclone Nargis (2008). *Geophys. Res. Lett.,* **36,** L03817, doi:10.1029/2008GL035815.

Lyman, J. M., J. K. Willis, and G. C. Johnson, 2006: Recent cooling in the upper ocean. *Geophys. Res. Lett.,* **33,** L18604, doi:10.1029/2006GL027033.

Mainelli, M., M. DeMaria, L. K. Shay, and G. Goni, 2008: Application of oceanic heat content estimation to operational forecasting of recent Atlantic category 5 hurricanes. *Wea. Forecasting,* **23,** 3–16.

Merrill, R., 1988: Characteristics of the upper-tropospheric environmental flow around hurricanes. *J. Atmos. Sci.,* **45,** 1665–1677.

Montgomery, M. T., M. M. Bell, S. D. Aberson, and M. L. Black, 2006: Hurricane Isabel (2003): New insights into the physics of intense storms. Part I: Mean vortex structure and maximum intensity estimates. *Bull. Amer. Meteor. Soc.,* **87,** 1335–1347.

Perlroth, I., 1967: Hurricane behavior as related to oceanographic environmental conditions. *Tellus,* **19,** 258–268.

Powell, M. D., P. J. Vickery, and T. A. Reinhold, 2003: Reduced drag coefficient for high wind speeds in tropical cyclones. *Nature,* **422,** 279–283.

Price, J. F., 1981: Upper ocean response to a hurricane. *J. Phys. Oceanogr.,* **11,** 153–175.

——, R. A. Weller, and R. Pinkel, 1986: Diurnal cycling: Observations and models of the upper ocean response to diurnal heating, cooling, and wind mixing. *J. Geophys. Res.,* **91,** 8411–8427.

Pun, I. F., I. I. Lin, C. R. Wu, D. S. Ko, and W. T. Liu, 2007: Validation and application of altimetry-derived upper ocean thermal structure in the western North Pacific Ocean for typhoon intensity forecast. *IEEE Trans. Geosci. Remote Sens.,* **45** (6), 1616–1630.

Roemmich, D., S. Riser, R. Davis, and Y. Desaubies, 2004: Autonomous profiling floats: Workhorse for broadscale ocean observations. *J. Mar. Technol. Soc.,* **38,** 31–39.

Shay, L. K., G. J. Goni, and P. G. Black, 2000: Effects of a warm oceanic feature on Hurricane Opal. *Mon. Wea. Rev.,* **128,** 1366–1383.

Trenberth, K., 2005: Uncertainty in hurricanes and global warming. *Science,* **308,** 1753–1754.

——, 2006: The role of the oceans in climate. NOAA annual report on the state of the ocean and the ocean observing system for climate, NOAA/Climate Program Office, Silver Spring, MD, 27–33.

Vecchi, G. A., and B. J. Soden, 2007: Effect of remote sea surface temperature change on tropical cyclone potential intensity. *Nature,* **450** (7172), 1066–1070.

Vimont, D. J., and J. P. Kossin, 2007: The Atlantic meridional mode and hurricane activity. *Geophys. Res. Lett.,* **34,** L07709, doi:10.1029/2007GL029683.

Wang, Y., and C. C. Wu, 2003: Current understanding of tropical cyclone structure and intensity changes—A review. *Meteor. Atmos. Phys.,* **87,** 257–278, doi:10.1007/s00703-003-0055-6.

Willis, J. K., J. M. Lyman, G. C. Johnson, and J. Gilson, 2007: Correction to "recent cooling of the upper ocean." *Geophys. Res. Lett.,* **34,** L16601, doi:10.1029/2007GL030323.

Wu, C.-C., C.-Y. Lee, and I.-I. Lin, 2007: The effect of the ocean eddy on tropical cyclone intensity. *J. Atmos. Sci.,* **64,** 3562–3578.